



SURGE-YAW CONTROL OF A HYBRID UNDERWATER ROBOTIC VEHICLE

Juan Carlos Cutipa Luque

Juan Pablo Julca Avila

Federal University of ABC

Av. dos Estados, 5001. Bairro Bangu. CEP 09210-580. Santo André - SP - Brazil.

juan.luque@ufabc.edu.br; juan.avila@ufabc.edu.br

Abstract. An underwater robotic vehicle is being developed at the UFABC (Universidade Federal do ABC) which has as main mission the inspection of ship hull thickness using ultrasonic transducers. This is a hybrid ROV (Remotely Operated Vehicle) due to its extreme locomotion capabilities adapted of the terrain tracked vehicles. This paper presents the surge-yaw control system of a new hybrid underwater vehicle that has two operation modes: free-flight and crawling. The free-flight mode uses a set of thrusters and the crawling mode uses two motorized tracks. The adherence between tracks and ship hull is guaranteed by applying a force normal to the hull surface from vertical thrusters. The conventional PID approach is used in order to control the horizontal dynamics composed of three degrees of freedom. The generated control signals are used to command the two thrusters to move the vehicle in the free-flight mode, and to command the two DC motors to move tracks of the crawling mode. The controlled vehicle responses are shown by numerical results focused to guarantee the performance specifications of the challenging and typical maneuvers.

Keywords: Underwater robotic vehicle, PID control, hybrid ROV, Ship inspection task.

1. INTRODUCTION

Offshore industry uses underwater vehicles to support drilling process, riser maintenance, ducts inspections, and other typical tasks performed at underwater environment. However, hybrid vehicles is the new trend in underwater systems due to their extreme capabilities required to accomplish challenge missions like a hull inspection of ships, platforms, and other offshore structures. In Brazil, the submarine activities have increased mainly by the interest in oil and gas production offshore industry. The recent discovers of pre-salt, located in deep waters, put Brazil in an attractive and prominent position, attracting the interest of the offshore industries, but the actual scenario presents also new challenges for engineering and research. Eventually, the adaptation or hybridization of new technologies will overcome these challenges.

In former works, the authors have been involved with modeling, identification and control systems of Remotely Operated Vehicles (ROVs) and Autonomous Underwater Vehicles (AUVs) (Cutipa-Luque and Donha, 2011; Avila *et al.*, 2013). There is a little number of hybrid underwater vehicles, which commonly combine ROV and AUV capabilities and operate in ultra-deep waters (Whitcomb *et al.*, 2010). A new hybrid underwater vehicle is under construction in the laboratories of the Federal University of ABC. This vehicle, defined as a Hybrid Remotely Operated Vehicle (HROV), combines capabilities found in ROVs and tracked terrain vehicles (Wong, 2001). The tracked systems are adapted from terrain tracked vehicles and provide extreme locomotion over the terrains at different soils properties (Liu and Liu, 2009). The HROV adopts a tracked system to provide the crawling motion over the ship hull and other offshore structures that remain semi-submerged at sub-sea.

A number of control approaches have been used to ensure the performance specifications due to the vehicle operates in hostile environment, subjected to waves, currents and noise sensors (Roberts and Sutton, 2006). Maurya *et al.* (2006) controlled successfully a torpedo shape AUV through the classical Linear Quadratic Regulator (LQR) approach. Silvestre and Pascoal (2007) designed a decoupled control system for an autonomous underwater vehicle based on the \mathcal{H}_∞ approach (Skogestad and Postlethwaite, 2005). Roche *et al.* (2011) presented a \mathcal{H}_∞ robust control for an autonomous underwater vehicle in which the control goal of the system remains guaranteed despite the measurement sensors presented varying parameters in sampling. Cutipa-Luque *et al.* (2012) presented the implementation of \mathcal{H}_∞ for an underwater vehicle torpedo shape where the AUV dynamics and motions are decoupled. The tuning process of advanced controllers is not as straightforward as tuning process of classical PID controllers. In (Whitcomb *et al.*, 2003), the authors applied the model-based adaptive PID approach (Slotine and Li, 1987) to tackle the control problem of a ROV. The current work presents the control of a HROV in surge and yaw directions based on conventional PID control approach (Åström and Hägglund, 2006).

The paper is organized as follows: section 1 presents the introduction of hybrid underwater vehicles and control approaches implemented in underwater vehicles; section 2 presents the mathematical model of the HROV included the tracked system; section 3 presents the design of conventional PID control technique for the HROV; section 4 presents the results of control approaches proposed where the responses, linear and nonlinear, are assessed through numerical simulations. Finally, section 5 presents the conclusions of the work and further experimental activities and researches.

2. UNDERWATER ROBOTIC VEHICLE MODEL

The HROV is described in Fig. 1 and consists of a mechanical structure made of polypropylene plates. The vehicle of 125 kg mass presents a rectangular parallelepiped shape with 1.08 m length, 0.57 m height and 0.83 m width. The whole HROV structure follows a modular design and can be easily reconfigured. At the top side, a polypropylene floatation box is installed to compensate and guarantee hydrostatic stability. The underwater vehicle has a pressure vessel for electronics embedded boards and inertial navigation sensors. The actuators are composed of a set of four vertical thrusters, two horizontal thrusters, and two horizontal tracks powered independently by two DC electric motors. DVL sensor and Depthmeter sensor are also installed at the bottom side. An umbilical cable is used for electric power supply and data transmission, and is connected to an isolated 4.5 kW DC power supply. The Fig. 2 presents the actual hybrid ROV under final stage of construction. A complete and detailed description of the HROV, mechanical design, electronics, sensors and actuator technical specifications, will be presented shortly in a further paper.

Figure 3 presents the body frame coordinates of the vehicle defined by the surge u , sway v and heave w linear velocities. Three angular velocities relative to the linear velocities are defined respectively as roll p , pitch q , and yaw r . The external forces are represented by capital letters X , Y , Z , K , M , N , respectively. Moreover, an inertial frame is defined by the position x , y and z and attitude ϕ , θ and ψ , which are used to locate the vehicle over the sub-sea environment (Fossen, 2002). In this paper, the aim is to control the vehicle in horizontal dynamics u , v and r using controllers, which feed control signals to the two horizontal thrusters and two motorized tracks. The vehicle moves at constant speeds in heave $\dot{w} = 0$, roll $\dot{p} = 0$ and pitch $\dot{q} = 0$.

This is a hybrid ROV where the two operation mode models differ in external forces applied over the system. The free-flight model represents the dynamics when the vehicle navigates free under the sub-sea and the crawling model represents the dynamics when the vehicle moves attached to the ship hull. The free-flight dynamic model of the HROV can be expressed using the standard equations for ROVs (Fossen, 2002):

$$M\dot{v} + C(v)v + D(v)v + g(\eta) = \tau, \quad (1)$$

where v represents the velocity vector, M represents the mass matrix, $C(v)$ represents the Coriolis matrix, $D(v)$ represents the damping matrix, $g(\eta)$ represents the hydrostatic force vector, and τ represents the control vector. Equation (1) represents a multivariable system where the matrix orders are determined by the degree-of-freedom (DOF) of the underwater vehicle motions. A complete dynamic model of the vehicle can be determined from its three longitudinal (surge, sway and heave) and its three angular (roll, pitch and yaw) motions to merge into a model of 6-DOF. It is assumed that the vehicle model deals with surge velocity (u), sway velocity (v) and yaw rate (r) dynamics merging into a model of 3-DOF in which the vectors and matrices are expressed as follows:

$$v = [u \quad v \quad r]^T, \quad (2)$$

$$M = M_{RB} + M_A, \quad (3)$$

$$M_{RB} = \begin{bmatrix} m & 0 & -my_g \\ 0 & m & mx_g \\ -my_g & mx_g & I_z \end{bmatrix}, \quad (4)$$

$$M_A = \begin{bmatrix} -X_{\dot{u}} & 0 & 0 \\ 0 & -Y_{\dot{v}} & 0 \\ 0 & 0 & -N_{\dot{r}} \end{bmatrix}, \quad (5)$$

$$C(v) = C_{RB}(v) + C_A(v), \quad (6)$$

$$C_{RB}(v) = \begin{bmatrix} 0 & 0 & -m(x_g r + v) \\ 0 & 0 & mu \\ m(x_g r + v) & -mu & 0 \end{bmatrix}, \quad (7)$$

$$C_A(v) = \begin{bmatrix} 0 & 0 & Y_{\dot{v}}v \\ 0 & 0 & -X_{\dot{u}}u \\ -Y_{\dot{v}}v & X_{\dot{u}}u & 0 \end{bmatrix}, \quad (8)$$

$$D(v) = \begin{bmatrix} -X_{|u|}u & 0 & 0 \\ 0 & -Y_{|v|}v & 0 \\ 0 & 0 & -N_{|r|}r \end{bmatrix}, \quad (9)$$

$$g(\eta) = [0 \quad 0 \quad 0]^T, \quad (10)$$

$$\tau = \begin{bmatrix} \tau_u \\ 0 \\ \tau_r \end{bmatrix} = \begin{bmatrix} \tau_1 + \tau_2 \\ 0 \\ -y_{P1}\tau_1 - y_{P2}\tau_2 \end{bmatrix}, \quad (11)$$

where $M_{RB}(v)$ and $C_{RB}(v)$ are the mass matrix and Coriolis matrix components, respectively, due to rigid body dynamics; $M_A(v)$ and $C_A(v)$ are the added mass matrix and Coriolis added matrix components, respectively, due to the added mass hydrodynamics; $X_{\dot{u}}$, $Y_{\dot{v}}$, and $N_{\dot{r}}$ are the added mass hydrodynamic terms that can be computed using strip theory or by aid of computer software; $X_{|u|u}$, $Y_{|v|v}$, and $N_{|r|r}$ are the damping terms due to the hydrodynamic drag that can be computed using commercial software of CFD (Computational Fluid Dynamic); τ_u is the resultant force and τ_r is the resultant moment due to the thruster actuator forces, τ_1 and τ_2 . Moreover, m is the mass of the vehicle, x_g and y_g are the location of mass center relative to a body reference frame located at the geometric center of the vehicle, y_{P1} and y_{P2} are the coordinates of the thrusters relative to the body frame. The drag coefficients of the HROV can be determined using FLUENT (a commercial computational fluid dynamic software) following the procedures given in (Avila *et al.*, 2013).

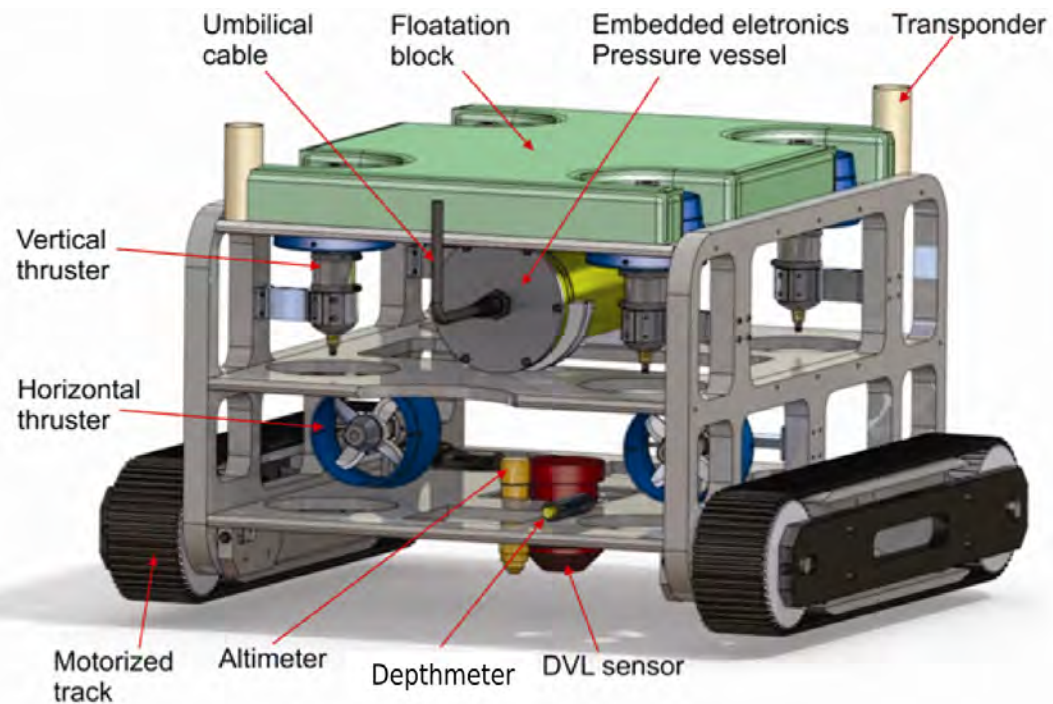


Figure 1: Hybrid Remotely Operated Vehicle (HROV).

The HROV took the extreme dynamics capabilities found in tracked terrain vehicles for crawling over the surface of the ship hull. Figure 4 presents the body forces actuating on the tracked system of the underwater vehicle. Friction forces are modeled according to the Coulomb's law of friction. Therefore, the forces and moments relatives to the track system can be modeled according to the following equations:

$$\begin{bmatrix} X_e \\ Y_e \\ N_e \end{bmatrix} = - \underbrace{\begin{bmatrix} R_{e1} + R_{e2} \\ \mu_v N \\ (-R_{e1} + R_{e2}) \frac{d_e}{2} + M_e \end{bmatrix}}_{\Gamma_e} + \underbrace{\begin{bmatrix} \tau_{e1} + \tau_{e2} \\ 0 \\ (-\tau_{e1} + \tau_{e2}) \frac{d_e}{2} \end{bmatrix}}_{\tau_e}, \quad (12)$$

where X_e is the resultant force over the tracks in surge direction, Y_e is the resultant force over the tracks in sway direction, and N_e is the resultant moment in yaw direction, N is the normal force perpendicular to the ship surface, R_{e1} and R_{e2} are the friction track forces and each one modeled by the expression $\mu_u N/2$, μ_u is the longitudinal friction coefficient, μ_v is the lateral friction coefficient, d_e is the distance between centerlines of the tracks, M_e is the moment turning resistance modeled by expression $\mu_v N l_e/4$ (Wong, 2001), τ_{e1} is the actuator force generated by track 1 and τ_{e2} is the actuator force generated by track 2. The normal force N is proportional to the maximum traction force (Bekker, 1969). Different to the terrain tracked vehicles where the normal force is a weight constant, here, the normal force is defined as the hydrostatic normal force, straightforward computed from roll and pitch angles, plus the applied vertical thruster forces, as shown below:

$$N = (W - B) \cos \theta \cos \phi + \tau_3 + \tau_4 + \tau_5 + \tau_6, \quad (13)$$

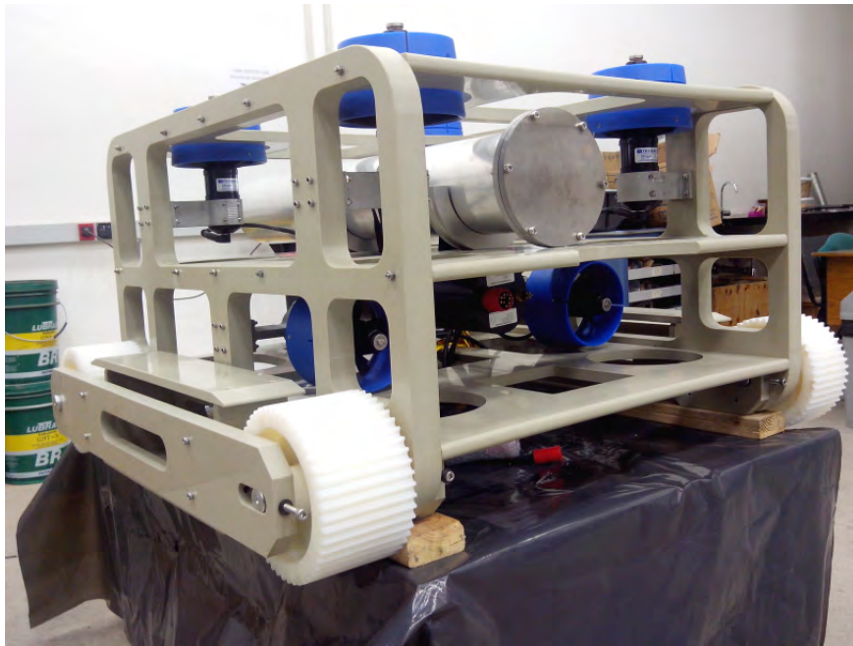


Figure 2: Hybrid ROV under final stage of construction.

where $W = mg$ is the weight of the vehicle, B is the Buoyancy force, and the forces of vertical thrusters are represented by τ_3, τ_4, τ_5 and τ_6 . Considering $W \approx B$, the maximum force of traction will be determined by thruster vertical actuators. In this paper, the normal force was set to a constant, and each force of vertical thrusters sets to 50 N. The maximum traction force F_{max} can be computed from the contact area of the tracks A_e over the ship hull, the cohesion coefficient c_e between the tracks and the hull of a ship, and shear resistance angle α_s (Bekker, 1969):

$$F_{max} = A_e c_e + N \tan \alpha_e. \quad (14)$$

The coefficients c_e and α_e will be determined through experimental tests in further and, if necessary, the values of vertical thruster forces shall be increased in order to guarantee good traction in the tracks. An excessive value of normal force increases the turning resistance M_e , which opposes to the motion and reduces the maneuverability of the vehicle.

The track traction forces are generated using DC motors and a first order filter can straightforward represent each DC motor. However, this work neglected the DC motor dynamics in order to reduce the complexity in assessing the control approach and the results focuses in terms of effort required by tracked system. Finally, considering the friction track force vector Γ_e and the control track vector τ_e , the 3-DOF crawling dynamic model of the hybrid ROV can be expressed as:

$$M\dot{v} + C(v)v + D(v)v + g(\eta) + \Gamma_e = \tau_e. \quad (15)$$

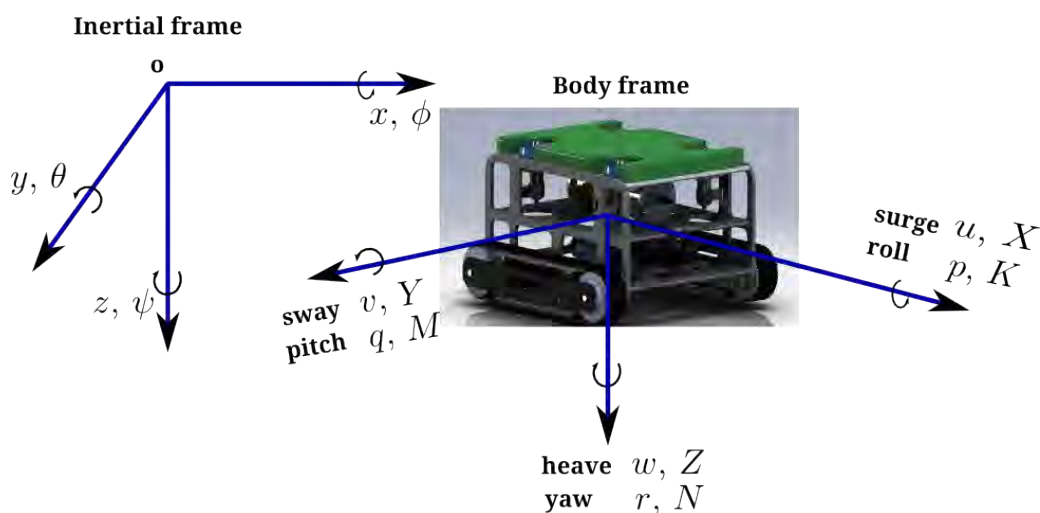


Figure 3: Coordinate systems of the HROV: inertial and body frames.

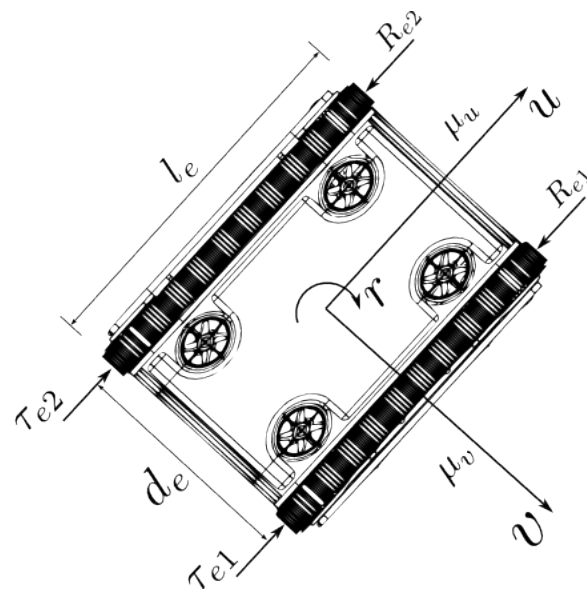


Figure 4: Track system forces of the underwater robotic vehicle (top view).

3. CONTROL SYSTEM

The HROV operates in two operation modes to perform the inspection task of a ship hull. A set of four controllers are synthesized, grouped in two couples. A first couple of controllers are synthesized for free-flight mode to carry the vehicle close to the hull ship. A second couple of controllers are synthesized for crawling mode to maneuver the vehicle over the hull of a ship. Initially, the free-flight controllers are used to carry the vehicle close to the hull ship. The crawling controllers are activated after the vehicle is attached¹ to the hull of a ship. The free-flight mode is powered only by the two horizontal thrusters and the crawling mode is powered only by the two motorized tracks. This paper deals with the design of controllers for the two operation modes of the vehicle considering the 3-DOF. The classical Proportional Integral Derivative (PID) control approach is used with its variants, Proportional Derivative (PD) and Proportional Integral (PI). Because the synthesis process is based on linear time model, the 3-DOF dynamic model expressed in Eqs. (1) and (15) will be linearized around a cruise speed and decoupled in particular motions.

Figure 5 presents the structure of the control design for the underwater vehicle. The control syntheses are accomplished using decoupled models as surge motion as yaw angle motion.

The control architecture of the HROV has been designed for providing fast deployment of data acquisition, control systems and, state estimation and navigation systems. This is based on a PC-104 single-board computer running the VxWorks real time operating system. This paper deals with surge and yaw control for a 3-DOF HROV model which allows to accomplish maneuvers in horizontal plane relative to the body frame. Control system of heave and pitch will be developed and presented in further works.

3.1 Surge control

The PI control is proposed in order to synthesize a controller the vehicle in the surge motion. The HROV model of Eq. (1) is decoupled and linearized in surge velocity u and expressed as:

$$(m - X_{\dot{u}})\dot{u} - X_u u = \tau_u, \quad (16)$$

where $X_u u$ is a linearized expression of $X_{|u|u}|u|u$ close to the cruise speed of the vehicle. Equation (16) can be transported to the Laplace s domain and represented by its gain k and time constant T parameters:

$$\frac{u}{\tau_u} = \frac{k}{Ts + 1}, \quad (17)$$

where $k = -1/X_u$ and $T = -(m - X_{\dot{u}})/X_u$. The control law can be expressed as (Åström and Hägglund, 2006):

$$\tau_u = -(K_P \tilde{u} + K_I \int_0^t \tilde{u} dt), \quad (18)$$

¹The maneuver of the attachment is complex and will be accomplished with the support of additional proximity sensors installed in the vehicle and with heave and pitch controllers that will be presented in further works.

where K_P is the proportional gain and K_I is the integral gain of the PI controller. The closed loop equation is expressed as follows:

$$T\ddot{u} + (1 + kK_P)\dot{u} + kK_I u = kK_P \dot{u}_{ref} + kK_I u_{ref}, \quad (19)$$

where u_{ref} is the reference command signal. The location of closed loop complex poles will determine the controlled system response. Moreover, in Laplace domain, the transfer functions in open loop L and in closed loop C result:

$$L = \frac{kK_I \left(\frac{K_P}{K_I} s + 1 \right)}{s(Ts + 1)}, \quad (20)$$

$$C = \frac{\left(\frac{K_P}{K_I} s + 1 \right)}{\left(\frac{T}{kK_I} s^2 + \frac{1 + kK_P}{kK_I} s + 1 \right)}. \quad (21)$$

The parameters of the controller can be tuned using the root locus method, fixing a rate for $K_I/K_P > 1/T$ and computing the integrator gain K_I from the root locus plot of L . Another straightforward alternative is to use the pole allocation from the closed loop C or the Eq. (19). The parameters of the PI controller for the surge motion can be found following the relations below:

$$K_I = \frac{\omega_n^2 T}{k} > 0, \quad (22)$$

$$K_P = \frac{2\zeta K_I}{\omega_n} - \frac{1}{k} > 0, \quad (23)$$

where ζ is the damping coefficient and ω_n is the natural frequency of the controlled feedback system.

3.2 Yaw control

The HROV model of Eq. (1) is decoupled and linearized in sway velocity v and yaw rate r directions, and expressed as a second order Nomoto model:

$$\frac{r}{\tau_r} = \frac{k(T_3 s + 1)}{(T_1 s + 1)(T_2 s + 1)}, \quad (24)$$

where T_* are the time constants and k is the gain of the system. The above model can be reduced to a first order model:

$$\frac{r}{\tau_r} = \frac{k}{(T s + 1)}, \quad (25)$$

where $T = T_1 + T_2 - T_3$ is the new constant time. Considering the kinematic equation of yaw angle $\dot{\psi} = r$, the model can be expressed as:

$$T\ddot{\psi} + \dot{\psi} = k\tau_r, \quad (26)$$

The control system can be represented following the PD law (Fossen, 2002):

$$\tau_r = -(K_P \tilde{\psi} + K_D \dot{\psi}), \quad (27)$$

where K_P is a constant relative to the proportional action, K_D is the derivative constant of the controller, $\tilde{\psi}$ is the error signal between the observed angular velocity $\dot{\psi}$ and the angular velocity reference signal $\dot{\psi}_{ref}$. The feedback system is then closed in loop and expressed as a typical second order system:

$$T\ddot{\psi} + (1 + kK_D)\dot{\psi} + kK_P\psi = kK_P\dot{\psi}_{ref}, \quad (28)$$

where $\dot{\psi}_{ref}$ is the command reference signal of yaw angle. The above equation is a second order differential equation where controller parameters can be obtained straightforward and are in function of natural frequency ω_n and damping coefficient ζ , as follows:

$$K_P = \frac{\omega_n^2 T}{k} > 0, \quad (29)$$

$$K_D = \frac{2\zeta\omega_n T - 1}{k} > 0. \quad (30)$$

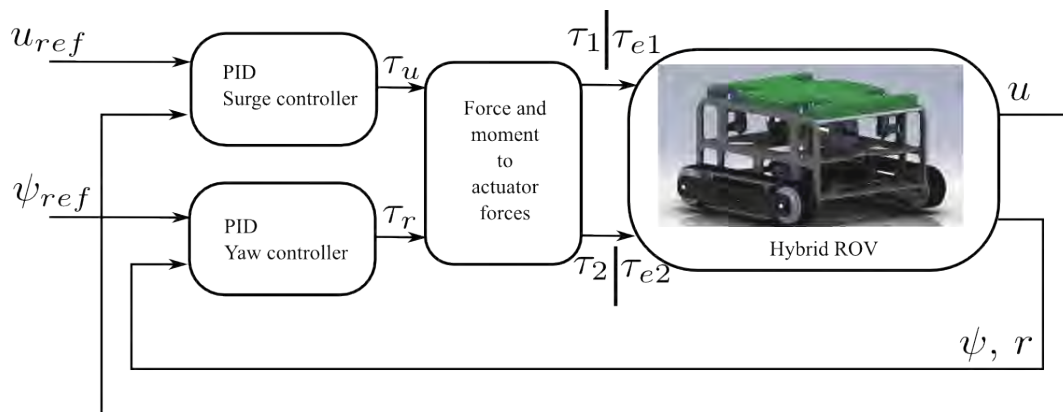


Figure 5: Surge-yaw control structure: thruster signals τ_1 and τ_2 are feed in free-flight mode and track signals τ_{e1} and τ_{e2} are feed in crawling mode.

The integral action $K_I \int_0^t \tilde{\psi}$ can even be added to the PID controller structure. However, the integral action are not necessarily an attempt because the model presents a pure integrator model by the relation between ψ and r to carry out the error signal to zero in steady state. According to the Fossen (1994), the integral gain K_I can be added and tuned following the relation:

$$K_I = \frac{\omega_n^3 T}{10k} > 0. \quad (31)$$

4. RESULTS

The controllers were designed to control a nonlinear dynamic model of the HROV in its 3-DOF. The performance of the feedback controlled system was assessed through numerical simulation and using Matlab. It is important to observe the controllers were synthesized based on a Linear Time Invariant models and some kind of information was lost in the process of linearizing and decoupling dynamics. Nevertheless, the controlled system will shall guarantee good stability, fast rise time responses, reduced overshoot, zero steady state error, and rejection to perturbation and model uncertainties. The control design specifications were summarized in below:

1. Stability;
2. Rise time < 7 seconds;
3. Overshoot < 25 percent;
4. Steady state error ≈ 0 ;
5. Rejection to output perturbation and model uncertainties.

Table 1 presents the parameters of the PID controllers. The PI controller for surge motion was straightforward to tune as for free-flight operation mode as for crawling operation mode. Two controllers are synthesized in order to perform maneuvers of ship hull inspection. The free-flight controller is used to maneuver the vehicle close to the hull ship. The crawling controller is activated after the underwater vehicle is attached to the hull ship and is moved through the two tracks.

Figure 6 presents the linear and nonlinear response of the controlled system in surge direction. The vehicle moves at surge speed of 0.5 m/s (Fig. 6a) meanwhile the yaw angle is keeping at 10 degrees (Fig. 6b). Figures 6c shows force and moment signals to be applied in surge and yaw directions. Figure 6d shows the thruster forces required by control actuator signals of the system. The difference between τ_1 and τ_2 is greater in transient and goes to zero in steady state, indicating that an initial moment should be generated through the variation of the thruster forces until reaching the desired angle value of 10 degrees and, after, the moment should be carried to zero value. The thruster forces are keeping at steady state constant values of 27.5 N, keeping a surge speed of 0.5 m/s.

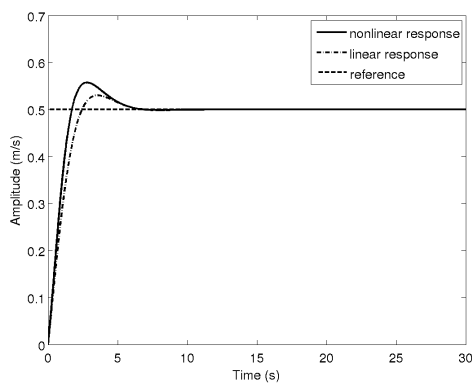
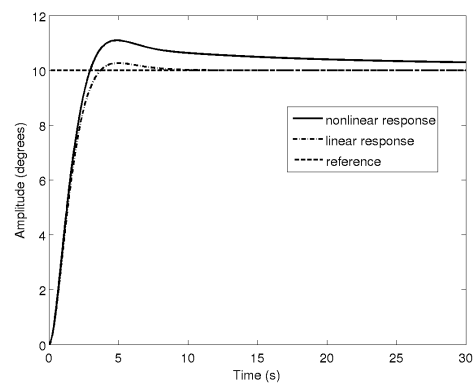
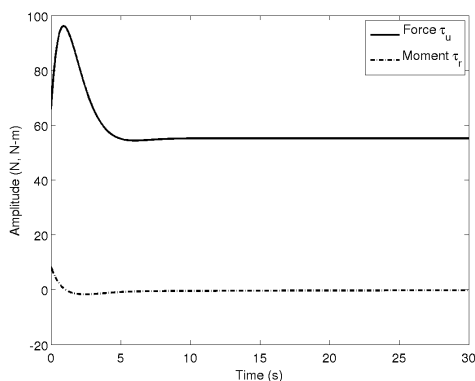
Figure 7 presents the response of the controlled system in crawling mode. The vehicle moves at surge speed of 0.5 m/s (Fig. 7a) meanwhile the yaw angle is keeping at 10 degrees (Fig. 7b). Figures 7c shows force and moment signals to be applied in surge and yaw directions. Figure 7d shows the thruster forces required by control actuator signals of the system. The difference between τ_1 and τ_2 , in contrast with free-flight mode, is greater in transient and goes to a constant value in steady state, indicating that an initial moment should be also generated with the variation of the thruster force until

reaching the desired angle value of 10 degrees and, after, the moment should be carried to a constant value compensating the friction moment relative to the tracked system.

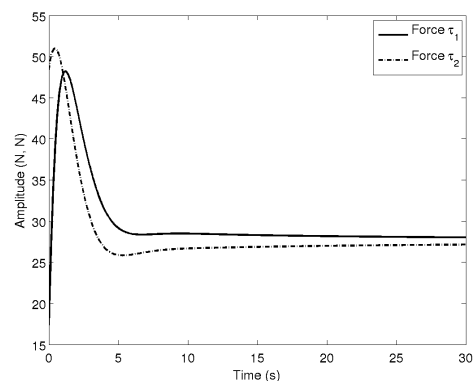
Turning resistance is present in this hybrid ROV vehicle due to the irregular distribution of lateral friction forces of the tracks and, as shown in terrain vehicles (Wong, 2001), a turning moment overcomes its effect. Figure 7d shows a steady state difference between track forces indicating the required turning moment for this maneuver. In free-flight mode (Fig. 6d), despite to be the same maneuver, the thruster forces reach to the same value in the steady state indicating the lack of turning moment. In fact, the turning resistance M_e appears only when the vehicle operates in crawling mode with its tracks attached to the hull of a ship. There are many semi-empirical models for turning resistance that can be also examined in further (Wong, 2001). Another better alternative is to use a maneuver data record with system identification methods in order to determine the model parameters (Cutipa-Luque and Donha, 2009).

Yaw controller parameters were not straightforward to tune due the responses presented large steady state errors that were tackled adding an integral action. Figure 8a presents the responses of the three crawling controller in the attempt of reducing rise time. The selected yaw controller that showed best performance ($\zeta = 0.7$ and $\omega_n = 1.5$) was submitted to model uncertainties tests, varying the friction coefficients between 40 % and 160 % of their settled values (see the Fig. 8b).

The stability of the system is achieved according to the Hurwitz, ensuring that all poles of the closed loop system remains in the Left Half Plane (LHP). The steady state error specification was also guaranteed for all responses. In all responses, the rise time was less than 7 s (Fig. 6 and Fig. 7), but it can slightly increase when the model is corrupted by model uncertainties (Fig. 8b).

(a) Surge velocity u response.(b) Yaw angle ψ response.

(c) Control actuator signals.

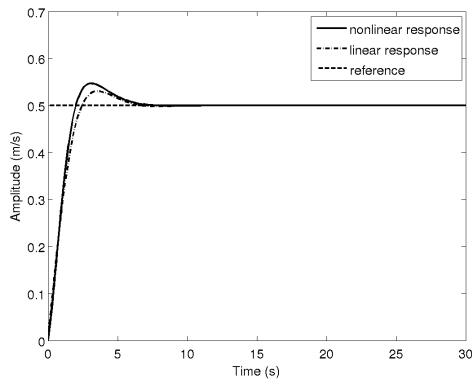


(d) Propeller actuator forces.

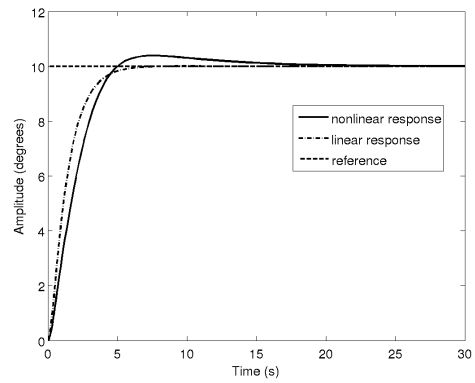
Figure 6: Surge-yaw control for the HROV: free-flight operation mode

5. CONCLUSIONS

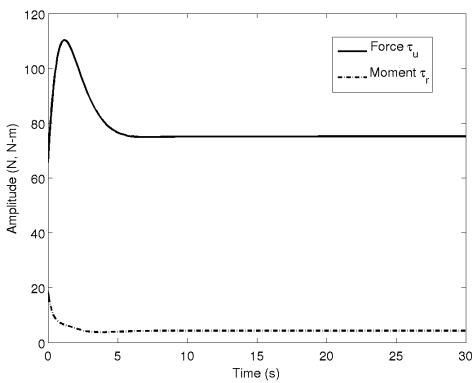
The current work dealt with control design for a new class of underwater vehicle in horizontal dynamics. A 3-DOF model of a hybrid vehicle was described in which the tracked system was adapted from the terrain tracked vehicles class. The PID controllers guaranteed the performance specifications. For the free-flight mode operation, a proportional-integral structure was used to control the vehicle in surge direction and a proportional-derivative structure was used to control the vehicle in yaw direction. For the crawling mode operation, a proportional-integral structure was used to control the vehicle in surge direction and a proportional-integral-derivative structure was used to control the vehicle in yaw direction.



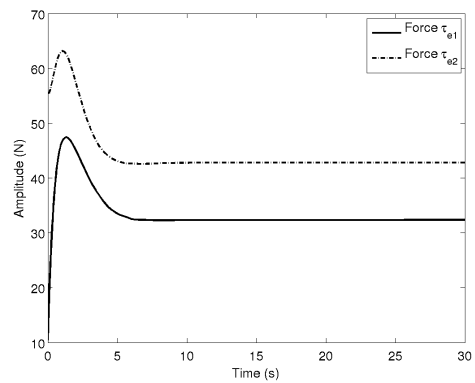
(a) Surge velocity u response.



(b) Yaw angle ψ response.

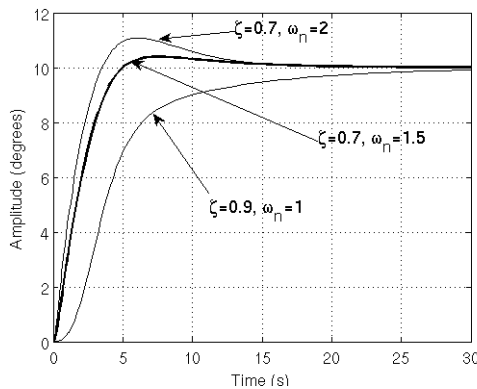


(c) Control actuator signals.

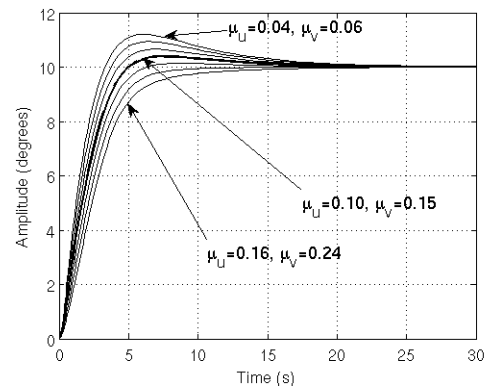


(d) Track forces.

Figure 7: Surge-yaw control for the HROV: crawling operation mode.



(a) Yaw angle ψ responses at different ζ and ω_n parameters.



(b) Yaw angle responses at different μ uncertainties.

Figure 8: Different parameters to pole allocation controller and controlled system responses subjected to uncertainties in friction Coulomb coefficients.

The friction forces relative to the tracked system cause steady state error in yaw direction and it was tackled using an integral action. The hybrid ROV controllers presented good performances and guaranteed time domain specifications included when parameter uncertainties are considered. Large values of friction parameters of the tracks can slightly increase the rise time. In crawling mode operation, the moment turning resistance requires additional control efforts. However, stability, steady state error and overshoot specifications remain between desired values. In a further work, these controllers will be validated through experimental tests and the results will be compared with other advanced robust control approaches in order to choose the better control system for this new hybrid underwater robotic vehicle.

Table 1: Surge-yaw PID Controller parameters

Operation mode	Surge controller					Yaw controller				
	ζ	ω_n	K_P	K_D	K_I	ζ	ω_n	K_P	K_D	K_I
Free-flight	0.7	1	131.84	—	229.71	0.7	1	47.04	61.14	—
Crawling	0.7	1	131.84	—	229.71	0.9	1	47.04	79.96	4.70
Crawling	0.7	1	131.84	—	229.71	0.7	1.5	105.84	143.46	15.88
Crawling	0.7	1	131.84	—	229.71	0.7	2	188.16	258.71	37.63

6. ACKNOWLEDGEMENTS

The authors would like to thank the FAPESP for financial support (under process number 2011/51955-5) and scholarship support, and the Windriver Inc. for the donation of the VxWorks operating system. The authors also would like to thank the Federal University of the ABC (UFABC) for scholarship support and laboratory facilities.

7. REFERENCES

- Åström, K. and Hägglund, T., 2006. *Advanced PID control*. ISA-The Instrumentation, Systems, and Automation Society; Research Triangle Park, NC 27709,.
- Avila, J.P.J., Donha, D. and Adamowski, J., 2013. “Experimental model identification of open-frame underwater vehicles”. *Ocean Engineering*, Vol. 60, pp. 81–94.
- Bekker, M.G., 1969. *Introduction to the Terrain-Vehicle Systems*. The University of Michigan Press.
- Cutipa-Luque, J.C., Dantas, D.L., de Oliveira, L. and de Barros, E.A., 2012. “Robust control of an underactuated auv”. In *The 9th IFAC Conference on Manoeuvring and Control of Marine Craft 2012*. Arenzano, Italy.
- Cutipa-Luque, J.C. and Donha, D.C., 2009. “Auv parameter identification”. In *Proceedings of the 8th IFAC Conference on Manoeuvring and Control of Marine Craft*. Poli-USP, Guarujá, Sao Paulo.
- Cutipa-Luque, J.C. and Donha, D.C., 2011. “Auv identification and robust control”. In *18th IFAC World Congress*. Milan, Italy, pp. 14735–14741.
- Fossen, T.I., 1994. *Guidance and Control of Ocean Vehicles*. John Wiley & Sons, West Sussex PO19 1UD, England.
- Fossen, T.I., 2002. *Marine control systems: guidance, navigation and control of ships, rigs and underwater vehicles*. Marine Cybernetics Trondheim,, Norway.
- Liu, Y. and Liu, G., 2009. “Track–stair interaction analysis and online tipover prediction for a self-reconfigurable tracked mobile robot climbing stairs”. *Mechatronics, IEEE/ASME Transactions on*, Vol. 14, No. 5, pp. 528–538. ISSN 1083-4435. doi:10.1109/TMECH.2009.2005635.
- Maurya, P., Desa, E., Pascoal, A., Barros, E., Navelkar, G., Madhan, R., Mascarenhas, A., Prabhudesai, S., Afzulpurkar, S., Gouveia, A., Naroji, S. and Sebastiao, L., 2006. “Control of the maya auv in the vertical and horizontal planes: Theory and practical results”. In *Proceedings of the 7th IFAC Conference on Manoeuvring and Control of Marine Craft*. Instituto Superior Técnico, Lisbon, Portugal.
- Roberts, G.N. and Sutton, R., eds., 2006. *Advances in Unmanned Marine Vehicles*. THE IEE, United Kingdom.
- Roche, E., Senname, O., Simon, D. and Varrier, S., 2011. “A hierarchical varying sampling h infinity control of an auv”. In *18th IFAC World Congress*. Milan, Italy, pp. 14729–14734.
- Silvestre, C. and Pascoal, A., 2007. “Depth control of the infante auv using. gain-scheduled reduced-order output feedback”. *Control Engineering Practice*, Vol. 15(7), p. 883.
- Skogestad, S. and Postlethwaite, I., 2005. *Multivariable Feedback Control: Analysis and Design*. John Wiley & Sons.
- Slotine, J.J.E. and Li, W., 1987. “On the adaptive control of robot manipulators”. *The International Journal of Robotics Research*, Vol. 6, No. 3, pp. 49–59.
- Whitcomb, L., Jakuba, M., Kinsey, J., Martin, S., Webster, S., Howland, J., Taylor, C., Gomez-Ibanez, D. and Yoerger, D., 2010. “Navigation and control of the nereus hybrid underwater vehicle for global ocean science to 10,903 m depth: Preliminary results”. In *Robotics and Automation (ICRA), 2010 IEEE International Conference on*. pp. 594–600. ISSN 1050-4729. doi:10.1109/ROBOT.2010.5509265.
- Whitcomb, L.L., Howland, J., Smallwood, D.A., Yoerger, D. and Thiel, T., 2003. “A new control system for the next generation of us and uk deep submergence oceanographic rovs”. In *Proceedings of the 1st IFAC Workshop on Guidance and Control of Underwater Vehicles*. Citeseer, pp. 137–142.
- Wong, J.Y., 2001. *Theory of Ground Vehicles*. John Wiley & Sons, 3rd edition. ISBN 0-471-35461-9.